CrystEngComm

Accepted Manuscript

ROYAL SOCIETY OF CHEMISTRY

www.rsc.org/crystengcomm

CrystEngComm

PAPER

One-step hydrothermal synthesis of carbonated hydroxyapatite porous microspheres with a large and uniform size regulated by L-glutamic acid

Received 19th April 2016,
Accepted 00th xx 20xx

DOI: 10.1039/x0xx00000x

www.rsc.org/

Mei-li Qi,[a,b] Jia Qi,[a,b] Gui-yong Xiao,[a,b] Kai-yuan Zhang,[a,b] Chen-yu Lu,[a,b] Yu-peng Lu*[a,b]

The understanding of the role of acidic amino acids in the synthesis of calcium of phosphate (Ca-P) may provide effective ways to the design of advanced biomaterials. In this work, by employing L-glutamic acid (Glu), a one-step hydrothermal synthesis of porous carbonated hydroxyapatite (CHA) microspheres with high purity, good uniformity, controllable morphology, and large particle size is proposed. The morphology is well controlled by adjusting the concentration of Glu and the hydrothermal treatment time. The presence of Glu alters the growth pattern of Ca-P products and leads to particles from ribbons to flower-like microspheres due to adsorption and subsequent inhibiting action of the active growth sites onto CHA's surface. It is established that the optimal condition having a predominance of uniform microspheres with an average diameter of about 64 μm is Glu concentration at 0.06 M (at a Ca^{2+}: PO_4^{3-}: Glu molar ratio of 10.8:6:15). The CHA microspheres may be possibly used as effective carriers for biomedical applications.

1. Introduction

Compared with irregular particles which may cause inflammatory reactions, spherical hydroxyapatite (HA) has become a hotspot study due to its superior flowability, good mechanical and physical properties, high protein absorption capacity and large specific surface area.[1, 2] Porous spherical HA materials with strong absorption ability due to the additional specific area will permit circulation of body fluids, increase the potential for firm attachment of living tissue and enable regeneration as rapidly as possible.[3] Therefore, porous HA microspheres are preferable to be used in sustained-release drug-delivery systems, bone graft substitutes in the field of tissue engineering and protein adsorption, protein chromatography, separation and purification, and so on.[1, 4-6] Moreover, HA microspheres with large diameter sizes will possess better dispersibility and more compatibility with body tissues when used in implants. Uniform microspheres present more predictable flowing properties during injection.[7]

Generally, HA spheres can be obtained by spray drying method,[8-10] microemulsion method,[11, 12] high temperature melting method,[13] and template-directed hydrothermal method.[5, 14, 15] Shi et al.[16] used chemical precipitation method to prepare nano-HA particles with diameters of 20 nm and 80 nm. Sun et al.[17] reported porous HA microspheres of 5~10 μm diameter utilizing gelatin as a binding agent by spray drying method. Qi et al.[18] hydrothermally synthesized HA microspheres with an average diameter of 10.7 μm by using Na_2EDTA as a nucleator.

However, the size of HA spheres described in literatures consist of nanoscale to several micros with unsatisfactory spherical degree, and information about spherical HA particulates of larger than 50 μm diameter are few. In addition, some inconveniences are brought due to the use of unhealthy organic solvents, multi-step and complicated processes, and the size distribution is rather broad. In this sense, the development of a simple and eco-friendly method for the fabrication of large-sized HA microspheres with uniform size and degree of sphericity is an ongoing process and remains a challenge.

Among the reported approaches to prepare CHA (carbonated HA) samples by the use of $Ca(NO_3)_2$-$(NH_4)_2HPO_4$-$(NH_2)_2CO$-HNO_3 system[19], CHA products commonly exhibit a ribbon-,[20] whisker-,[21] fiber-[4, 22-24] or plate-/hexagonal prim-/needle-like[25, 26] particle morphology. Previous studies[27, 28] have shown that amino acids could inhibit the growth of HA due to the adsorption on HA crystal surfaces through hydrogen bonds and electrostatic attraction, which possibly influence the morphological development of apatite crystals. Boanini et al[29] found that the presence of the amino acids affects the degree of crystallinity of the apatitic phase and favours osteoblasts proliferation. Sharma et al synthesized petal-like HA particles with the incorporation of glutamic acid (Glu)[30]. Inspired by the urea-assisted system and biomineralization, here we demonstrate a one-step hydrothermal synthesis of CHA porous microspheres through the hydrolysis of urea containing the nontoxic modifier, Glu. The diameter of the obtained microspheres ranges mainly from 20 to 200 μm. By carefully increasing the Glu concentration, we determine the growth stages of CHA from irregular fibers to uniform porous microspheres, and then to flower-like spherical aggregates. Both the influence of Glu concentrations and the hydrothermal

[a] Key Laboratory for Liquid-Solid Structural Evolution and Processing of Materials, Ministry of Education, Shandong University, Ji'nan, 250061, China.
[b] School of Materials Science and Engineering, Shandong University, Ji'nan, 250061, China.
[c] E-mail address: biosdu@sdu.edu.cn; Fax: +86-0531-88395966; Tel: +86-0531-88395966.

† Electronic Supplementary Information (ESI) available. See DOI:

treatment time on the phases, structure and particle size of the products are analyzed. As discussed earlier, even though there are many reports on HA microspheres, the synthesis of porous CHA microspheres with a large and uniform size is extremely challengeable and has been hardly reported. Hence in this study, we are particularly focused on the uniform growth of CHA microspheres in the presence of Glu. This kind of microspheres could find applicability in bone tissue regeneration, such as drug-controlled release matrices, injectable bone defect fillers, protein and gene delivery carriers, and so on.

2. Experimental

In a typical procedure, the aqueous solution of $Ca(NO_3)_2{\cdot}4H_2O$, and $(NH_4)_2HPO_4$ were mixed, followed by the addition of 1M urea solution, while the molar ratio of Ca/P was kept at 1.8. The initial pH values (ipHs) of the reactions were adjusted by 0.5 M HNO_3(aq). Various concentrations of L-glutamic acid were added to the solution. Then the solutions were transferred to Teflon-lined cylindrical stainless steel autoclaves and treated hydrothermally at 180°C. Finally, the resultant suspensions were washed thoroughly with deionized water and anhydrous ethanol, and dried in air at 80°C. The details on sample names and their synthesis conditions can be found in Table 1.

X-ray diffractometer (XRD, EMPYREAN, 45 kV, CuKα radiation, λ=1.5404 Å) and fourier transform infrared spectrometer (FTIR, NEXUS 670) were performed to identify the phase and functional groups of the obtained products. Field emission scanning electron microscope (FE-SEM, SU-70, 15 kV) equipped with an energy dispersive spectrometer (EDS) and high-resolution transmission electron microscopy (HRTEM, JEM-2100F, 200 kV) was used to observe the morphology and selected area electron diffraction (SAED) of the as-synthesized products. Before TEM observation, the product was dispersed ultrasonically in distilled water for 3 minutes. The particle size distribution (PSD) and mean particle size were measured by LS13320 laser diffraction particle size analyzer with distilled water as the dispersion medium.

Table 1 Experimental conditions of HA microspheres

Sample ID	Concentration of Glu (M)	ipH	Temperature (°C)	Time (h)
S1	0.004	3.5	180	10
S2	0.02	3.5	180	10
S3	0.04	3.5	180	10
S4	0.06	3.5	180	10
S5	0.08	3.5	180	10
S6	0.12	3.5	180	10
T1	0.06	3.5	180	0.5
T2	0.06	3.5	180	1
T3	0.06	3.5	180	15
P1	0.06	3.5	140	1
P2	0.06	3.5	160	1

3. Results and discussion

3.1 Phase analysis

Figures 1 and 2 display the diffraction patterns of all the samples by comparison with a standard database (JCPDS card 09-0432). All the peaks are readily indexable with the HA, indicating that both the addition of different amounts of Glu and the increase of hydrothermal treatment time have no adverse effect on the phase purity. It is worth pointing out that the more additive amount of Glu, the stronger diffraction intensity along the (002) direction and the weaker along the (300) direction. Besides, the intense peak shifts from (300) to (211) in Fig 1 suggests a preferential orientation growth of HA.[20, 31, 32] Previous studies have shown that the metastable phase of octacalcium phosphate ($Ca_8(HPO_4)_2(PO_4)_4{\cdot}\ 5H_2O$, OCP) will appear at the early stage when using the homogeneous precipitation method.[33, 34] The conversion of OCP to HA is observed at 140-150°C.[35, 36] The pH of the solution increases accompanied by hydrolysis of urea, which leads to the nucleation and growth of HA crystallites. To investigate the process of phase transformation during the precipitation of HA, temperature-dependent growth experiments have been carried out with the Glu concentration fixed at 0.06 M and hydrothermal time fixed at 1 h (see samples P1 and P2 in Table 1). Peaks corresponding to OCP phase crystals (JCPDS card 26-1056)[37, 38] appear after heating to 140°C, including the characteristic (100) reflection at 2θ=4.7° (Fig. 3a). When the reaction temperature increases to 160°C (Fig. 3b), HA is obtained as the predominant phase. Only a weak reflection peak at 4.7° of OCP exists in the final product, showing that the product undergoes a transformation into the HA phase. After 180°C of hydrothermal treatment (Fig. 2b), the (100) reflection of OCP disappears completely and only HA reflections are obtained from the resulting product, indicating that the transformation from the intermediate OCP phase to the stable HA phase. It reveals that the OCP to HA phase transition progresses steadily as a function of the temperature- rise periods.

It is known that CO_3^{2-} is a common impurity in HA which can be substituted by PO_4^{3-}.[19, 39, 40] Since carbonate is produced during the hydrolysis of urea in the synthesis process, the incorporation of certain amounts of CO_3^{2-} in HA crystallites is inevitable.[41] In FTIR spectra (Fig. 4), the products obtained under different hydrothermal times have similar patterns. The absorption bands appearing in the lower wavenumber region at 1030 and 960 cm^{-1} are attributed to PO_4^{3-} group of HA.[39] The absorption peaks around 3570 cm^{-1} and 632 cm^{-1} arise from the stretching and flexural mode of structural OH^-, respectively.[36] In addition, the broad and weak bimodal bands at 1453 and 1420 cm^{-1}, and the peak at 872 cm^{-1} are the characteristic vibrations of CO_3^{2-} group, suggesting that the CO_3^{2-} group substitutes the B-site of PO_4^{3-} group in the HA.[40, 41] The FTIR results further confirm that the as-synthesized products are all carbonated apatite phase and not stoichiometric apatite.

Table 2 Particle sizes of HA microspheres

Sample ID	d_{10} (μm)	d_{50} (μm)	d_{90} (μm)	Mean Size (μm)
T1	8.323	50.45	76.44	51.23
T2	8.464	52.37	88.23	54.08
S4	8.697	51.13	140.4	63.58
T3	6.738	32.83	72.62	40.74

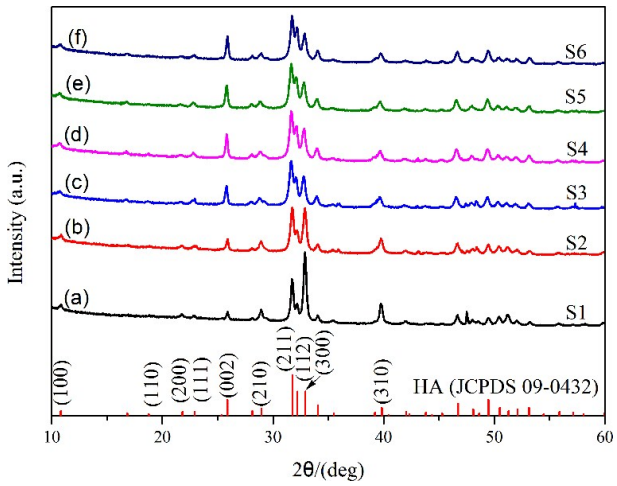

Fig. 1 XRD patterns of HA microspheres synthesized at 180°C for 10 h with different concentrations of Glu: (a) 0.004 M (b) 0.02 M (c) 0.04 M (d) 0.06 M (e) 0.08 M and (f) 0.12 M.

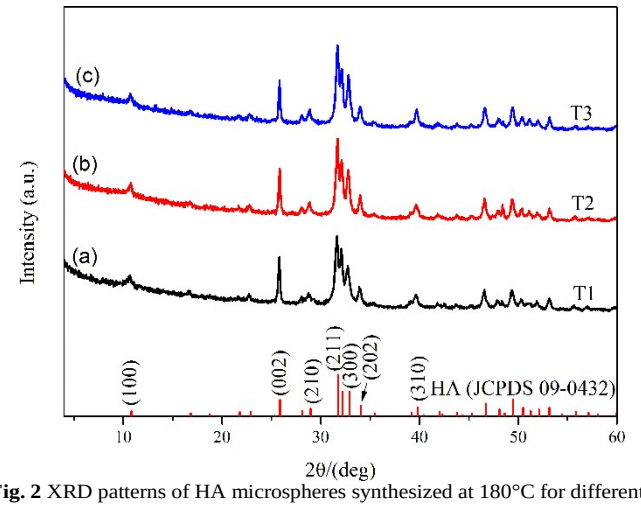

Fig. 2 XRD patterns of HA microspheres synthesized at 180°C for different hydrothermal times with 0.06 M Glu: (a) T1=0.5 h (b) T2=1 h and (c) T3=15 h.

Thus, in view of the XRD and FTIR results, the final crystals belong to CHA and the precursor is OCP. No extra impurity is found in the XRD and FTIR spectra.

3.2 Microstructural characterization

Figure 5 shows the SEM micrographs of the obtained products hydrothermally synthesized at 180°C for 10 h under ipH=3.5 with different contents of Glu, named S1 to S6. Obviously, the addition of Glu induces the changes in morphology of the resulted CHA particles. The morphology evolves from irregular fibers to well-developed porous microspheres with uniform sizes, and then to flower-like spherical aggregates. The sample S1 obtained with low addition of Glu (Fig. 5a) consists of irregular ribbon-like crystallites which are not uniform in length and width. When the concentration of Glu is increased to 0.02 M, the CHA fibers transform to urchin-like crystals with individual fibers radiating from the center (Fig. 5b). When Glu concentration at 0.04 M, flower-like regular assemblies of flakes transformed into porous microspheres (Fig. 5c). The diameter of CHA spheres are 20~100 μm. Extending Glu concentration to 0.06 M, in which Ca^{2+}: PO_4^{3-}: Glu molar ratio is 10.8:6:15, well-defined and smooth microsphere crystals were observed (Fig. 5d, sample S4). The microspheres become the dominate morphology of the products. As the addition of Glu continues to increase (Fig. 5e, f), the obtained particles are not spherical as shown in Fig. 5d. Besides, more flower-like aggregates appear, and the size uniformity of the microspheres becomes weaker with the diameter sizes range from about 20 to 140 μm (Fig. 5d~f). It is established that the optimal concentration of Glu having a predominance of uniform microspheres in this work is around 0.06 M.

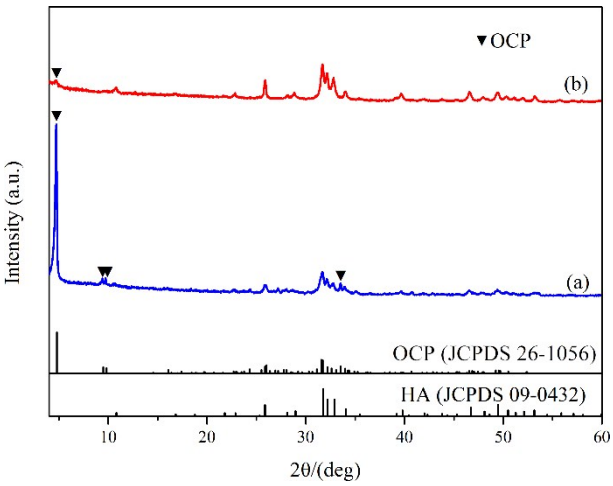

Fig. 3 XRD patterns of the evolution from OCP to HA phase at 1 h for different hydrothermal temperatures with 0.06 M Glu: (a) 140°C and (b) 160°C. Note the decrease in OCP intensity (100) reflection at 2θ=4.7° concomitant with the appearance of HA reflection in XRD.

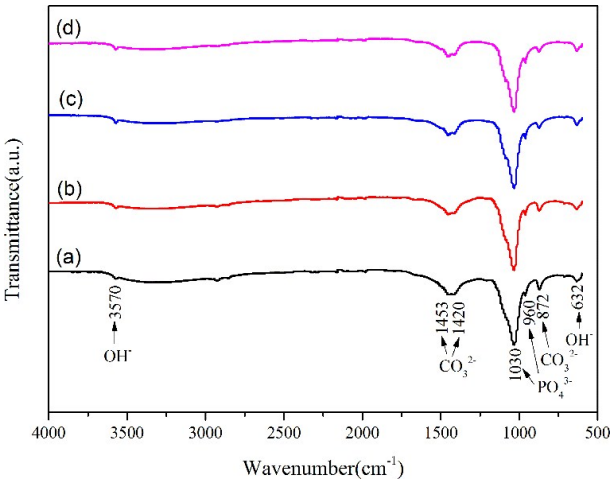

Fig. 4 FTIR spectra of the products synthesized at 180°C for different hydrothermal times with 0.06 M Glu: (a) 0.5 h (b) 1 h (c) 10 h and (d) 15 h.

Time-dependent growth experiments have been carried out with the Glu concentration fixed at 0.06 M to ascertain the details of the CHA crystallization process and observe the structure of HA at different growth times (see samples T1-T3 in Table 1). As the hydrothermal time increases, most of the products are spherical and the diameter of the CHA first increases and then decreases. At the early stage, microspheres with high spheroidization and uniformity are formed (shown in Fig. 6a). In continuation, the morphology does not change much as we

expected for some urchin-like particles (Fig. 6b). As the reaction time extends, some elementary porous microspheres grow much bigger and finally reach a diameter of ~100 μm (Fig. 6d). However, further increase of the hydrothermal treatment to 15 h results in the decrease in the size uniformity and total diameter of CHA microspheres (Fig. 6c). Additionally, irregular flower-like aggregates are increased.

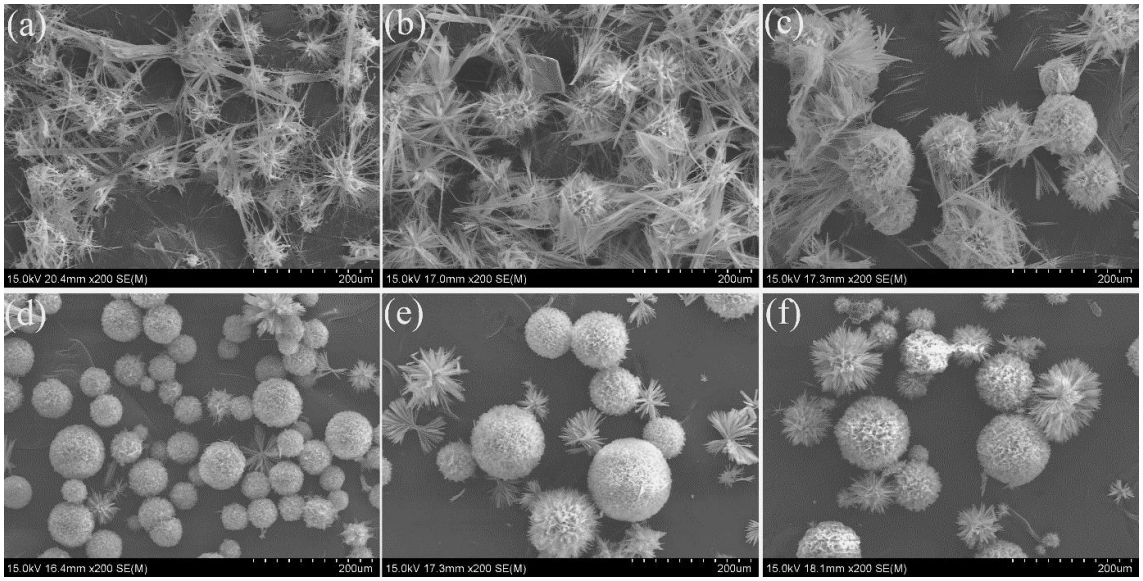

Fig. 5 SEM images of the as-obtained CHA synthesized with different concentrations of Glu at 180°C for 10 h (a) 0.004 M (b) 0.02 M (c) 0.04 M (d) 0.06 M (e) 0.08 M and (f) 0.12 M.

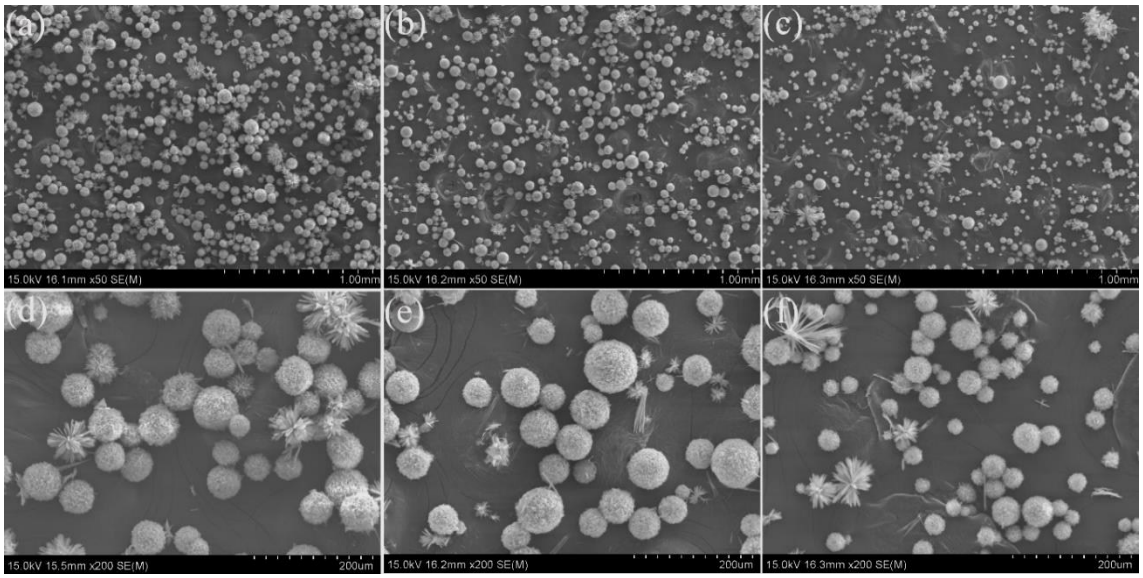

Fig. 6 SEM images of the as-obtained CHA microspheres synthesized at different hydrothermal times with Glu concentration fixed at 0.06 M: (a, d) 0.5 h (b, e) 1 h and (c, f) 15 h.

Figure 7 shows the morphology of a typical sphere in sample T1 at different magnification. The diameter of the porous sphere is about 70 μm and the average interconnected pore size of the microsphere is about 1.5 μm. The advantage of CHA with large pores, also called gigapores, is the rigidity.[42] Compared with other porous HA microspheres which are composed by flat flakes with a mesoporous structure,[5, 34, 43] the flakes are flexible and the pores are interconnected without cracks.

To further testify the transformation process from OCP to HA, the morphology and elemental analysis of the samples prepared at 1 h with 140°C and 160°C are characterized by FE-SEM equipped with EDS (Fig. 8). As the reaction temperature increases, the flower-like aggregates become spherical as shown in Figs. 8a and 8c. Two possible reasons are, (1) heat degradation of urea proceeds more at higher temperatures, (2) Glu promotes the spherical shape of aggregates and reduces the dimensions of the flowers during the temperature-rise period, particularly in the direction of the c-axis. From these results, it is indicated that reaction temperature over 160°C is beneficial to prepare the spherical HA particles. The EDS and elemental

analysis of the resultant powders in Figs. 8 b and 8d reveal the presence of Ca, P and O elements, corresponding to the XRD results in Fig. 3. (Elements for Al and Pt are caused by the use of aluminium foil during the sample preparation for FE-SEM). Besides, an appropriate increase in a Ca/P atomic ratio as calculated from the inset tables of spectrum curves. The Ca/P atomic ratio increases from 1.38 at 140°C to 1.47 at 160°C, in accordance with the transformation from OCP to HA, because the Ca/P ratio of OCP and HA is 1.33 and 1.67, respectively.

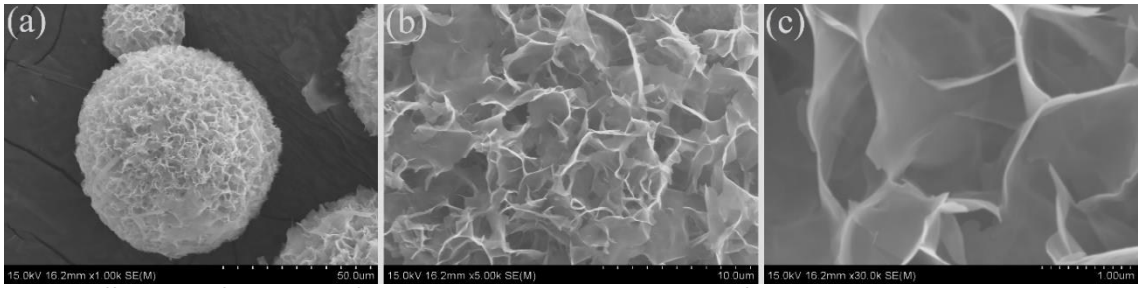

Fig. 7 SEM images at different magnification times of the as-obtained CHA synthesized at 180°C for 1 h with 0.06 M Glu.

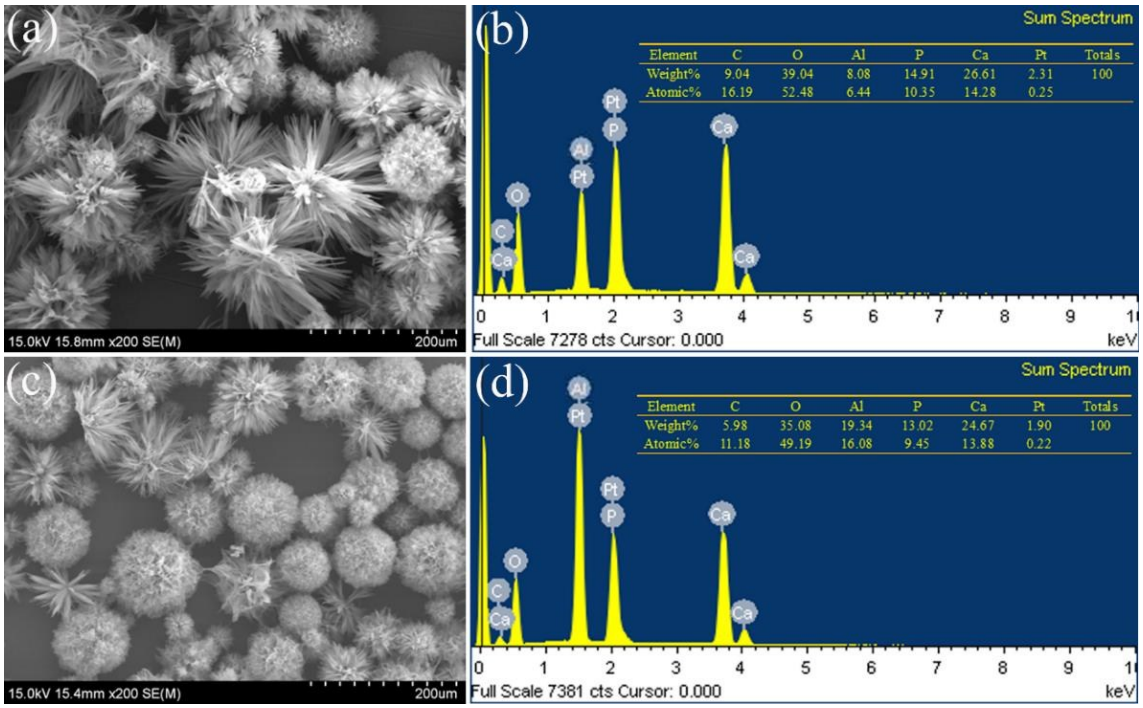

Fig. 8 SEM images and corresponding EDS of the products synthesized at 1 h for different hydrothermal temperatures with 0.06 M Glu: (a~b) 140°C and (c~d) 160°C

The crystal structure of the CHA powders for sample T1 is further analyzed by HRTEM (Fig. 9). Figure 7b shows the clear lattice fringes with interplanar spacing of 0.34 nm, which can be assigned to the (002) plane of the CHA crystal, indicating that the building units of the porous CHA microspheres are short fibers with longitudinal axis along (001] direction. Spots in the SAED (110) pattern near the (000) plane (Fig. 9c) are identified as (002), and (112), taken from the (-220) zone axis, and they match the vector relationship of the crystal planes. In other words, the addition of Glu does not alter the growth direction of CHA fibers. The role of Glu is just to inhibit the c-axis's growth of CHA which is discussed in literature,[44] thus the crystals grow along a-axis and b-axis to form spherical morphology. Besides, four distinct diffraction rings in Fig. 9d can be clearly assigned to the diffractions of the (002), (112), (212) and (004) planes of HA, further illustrating that the microspheres are indeed HA.

It can be inferred that the morphological changes are in agreement with the different relative intensities of diffraction peaks. As shown in Fig. 1, the relative intensity of (300) to (002) diffraction peaks decreases from sample S1 to S6. Sample S1 consists of individual and ribbon-like crystallites. A flat-lying orientation with the c-axis parallel to the XRD specimen surface is preferentially adopted, leading to strong (300) and weak (002) diffraction intensities. Meanwhile, when the morphology of the particles shifts to be spherical-like, fibers that are positioned with different radial directions contribute to an decreased (300) and increased (002) diffraction. It is reported that the adsorption behaviors of glutamate tend to occur on OCP's (100) planes and the adsorption behaviors may still exist after the transformation

of OCP to HA.[45] Koutsopoulos et al. have revealed that interactions of Glu with HA crystal surfaces lead to adsorption which follows a Langmuir's isotherm.[46, 47] In alkaline environment, the adsorption behaviors of Glu mainly occur on (100) planes due to the electrostatic forces, a-plane and b-plane of HA are inhibited and (100) planes of HA become more visible. This phenomenon results in inhibiting activity of Glu against HA crystal growth, thus fibers become shorter and spherical aggregates.

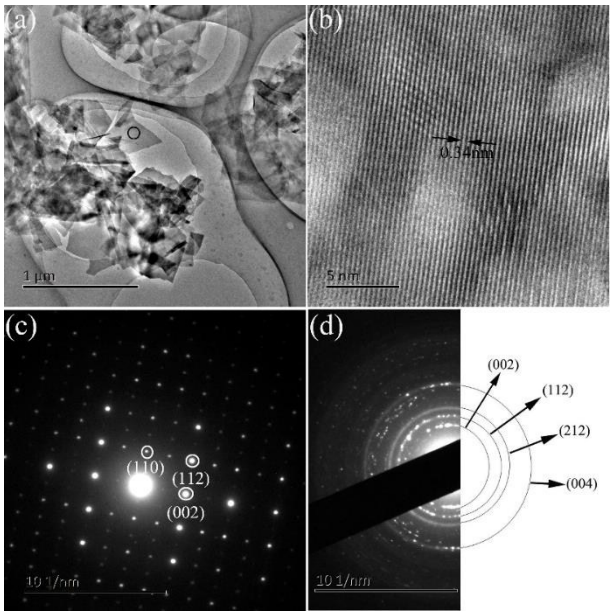

Fig. 9 TEM images of the as-obtained CHA synthesized at 180°C for 0.5 h (a) A typical image of the microsphere after ultrasound treatment, (b) the corresponding high resolution image and (c, d) the SAED pattern.

3.3 Size distribution

Particle size distribution is an important parameter influencing the property of CHA products. The granulometric analysis results of CHA microspheres are listed in Fig. 10 and Table 2. Figure 8 shows the particle size distribution curves of the CHA microspheres prepared at different times. It is found that except for the left shift of the main peak in T3, the particle sizes range is similar among T1, T2 and S4 with the corresponding size distributions mainly centers on 20~100 μm, indicating that the particle size of CHA microspheres does not change much with the increase of hydrothermal treatment time. The appearance of three main size peaks indicates the relatively uniform CHA microspheres. Besides, the curves show the large size of the obtained microspheres (60 μm). Table 2 shows that as the hydrothermal treatment time is increased from 0.5 h to 10 h, the mean particle sizes have a tendency to increase, from 51.23 to about 64 μm. However, when the hydrothermal treatment time increases to 15 h, a relatively great decrease appears in the mean sizes, which turns to be 40.74 μm.

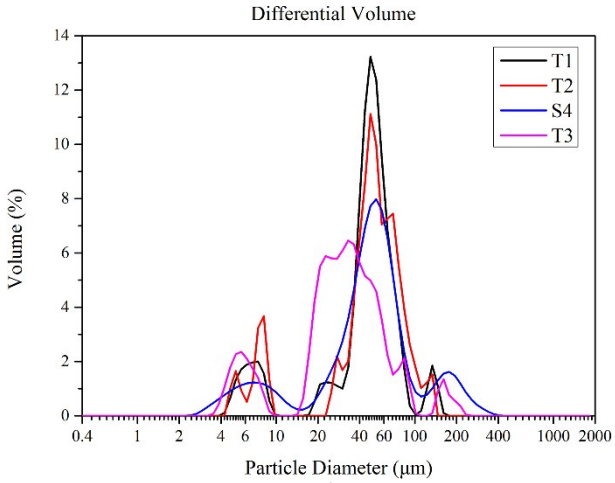

Fig. 10 Particle size distribution curves of the microspheres prepared at 180°C for different times with 0.06 M Glu.

3.4 Formation mechanism

Based on the experimental results and above discussion, a possible formation mechanism of well-developed CHA porous microspheres with a large and uniform size regulated by Glu under hydrothermal conditions is proposed. Fig. 11 illustrates the relationship between the diameter of the CHA microspheres and the experimental conditions. Aggregation of small crystal nuclei is accounting for the formation of spherical particles, being similar to the two step mechanism of yttrium hydroxycarbonate[48] and zinc sulphide spheres mechanism[49, 50], that is the formation of nuclei accompanied by aggregation of the crystallites to develop spherical particles composed of clusters. The porous structure of CHA microspheres may be attributed to both the effect of urea's rapid hydrolysis and Glu's inhibiting action of the active growth sites onto CHA's surface. Firstly, with the rapid hydrolysis of urea, high supersaturation is obtained and a large burst of nuclei occur in the bulk solution.[51] These nuclei grow sufficiently along (001) direction, resulting in long and irregularly sized ribbon-like crystals. The intrinsic crystal habit of HA caused by the lattice energy difference among different crystal planes leads to this kind of preferential growth.[9] Homogeneous precipitation with the presence of urea can be regarded as self-regulating because of the established equilibria between carbonic acid and ammonia released by urea decomposition.[52] Secondly, small addition of Glu changes the growth pattern of CHA crystallites. The ribbons tend to be shorter and spherical shapes begin to form. In this process, Glu plays a key role in inducing CHA fibers into growing directionally as a result of the interaction between OH^- and Ca^{2+} on the surfaces of CHA crystals and the morphological development of CHA crystals is thus influenced.[27, 53] Thirdly, with the addition of increasing Glu concentration, say 0.04 M in our experiment, the intense peak changes from (300) to (211) due to preferential growth[20, 31, 32] and the (002)/(300) intensity ratio is increased, accordingly the morphology becomes to be well-developed microspheres with diameters of 20~100 μm. It is expected that when the shape of the products changes to be more spherical-like, the ribbons positioned with different radial directions promote an decreased (300) and increased (002) diffraction intensities at respective planes.[15] An increase of the

peak intensity ratio I(300)/I(002) implies that growth along the c-axis is favoured.[54] Finally, with the increase of the Glu addition, the microspheres unfold and grow into urchin and bundle-like, which is resulted from the nonexistence of significant adsorption effect of Glu on CHA's crystal growth. It can be inferred that before the optimal concentration of Glu is reached, Glu promotes the spherical morphology of the CHA aggregates and reduces the dimensions of the blades, particularly in the direction of the c-axis and the uniformity of the microspheres is improved along with the increased Glu concentration. However, beyond the optimal concentration of Glu, the blocking action of Glu is weakened.

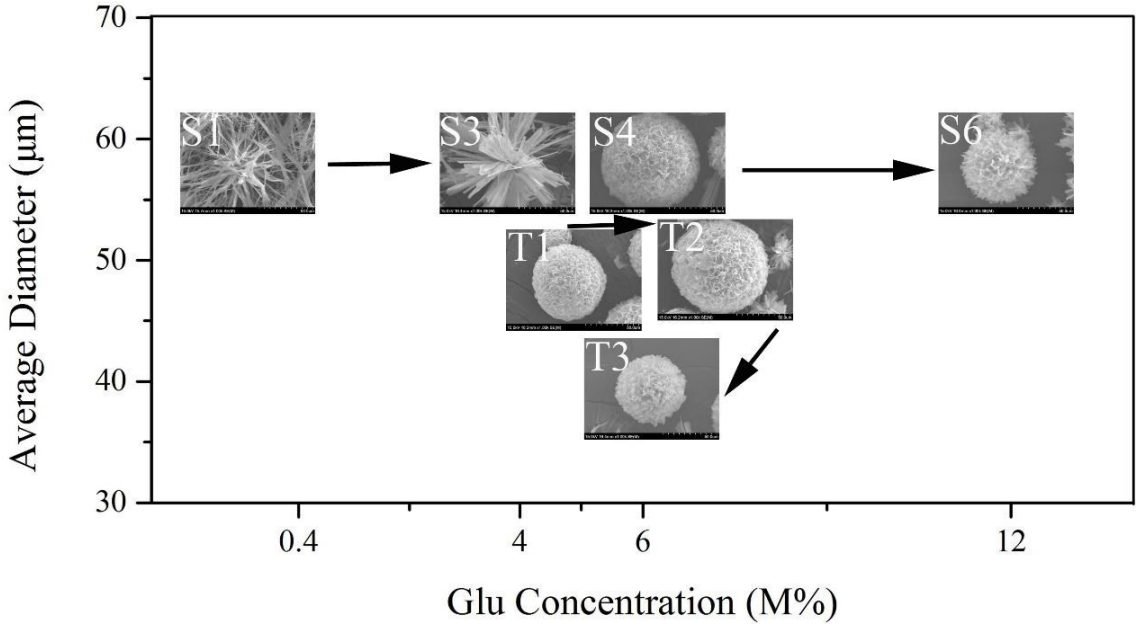

Fig. 11 Relationship between the diameter of the CHA microspheres and the experimental conditions. (The sample names are indicated in the corresponding SEM images.)

The whole process has two key points accounting for the large-sized microspheres. On the one hand, the gradual release of NH^{4+} produced by urea decomposition after heating above 80°C result in the relatively homogeneous pH field and provide the ''instant'' OH^- for CHA formation. One the other hand, the interaction of carboxyl groups of Glu with Ca^{2+} on the surfaces of CHA crystals lead to the formation of soluble complex. The subsequent hydrolysis of the complex make the slow rate release of Ca^{2+} possible. As the reaction proceeds, the driving force becomes higher, thus the interface produces a continuous growth.[36] After the formation of OH^- and Ca^{2+} by hydrolysis at the location of the former nuclei combine with the free PO_4^{3-} in the reaction system, the CHA start to grow microspheres with a large size. Compared to other methods of fabricating HA microspheres,[55] this simple process is advantageous to be conducted without toxic organic solvents or oils, thus enabling the recovery of spherical particles in the absence of sintering processes. Moreover, the obtained microspheres present a large and uniform size, even no need for a subsequent fractionation by sieving.

5. Conclusions

In summary, flower-like porous CHA microspheres with average diameter of about 64 μm are successfully prepared through a one-step hydrothermal method. Experimental results shows that the addition of Glu played a key role in controlling the morphology of the as-obtained products during formation of porous CHA microspheres. The well-developed microsphere crystals with regular morphology are observed with Glu concentration around 0.06 M and hydrothermal time at 10 h. Moreover, a possible formation mechanism of large-sized porous CHA microsphere is proposed. Such CHA material with porous, spherical and large-sized, should be highly dispersed and easy to be operated when used as separation mediums, filling materials, and cell carriers. In future research, the uniformity of size distribution and morphology will be further promoted and the in-vitro cell cultures and in-vivo animal experiments of such large-sized porous CHA microspheres will be conducted.

Acknowledgements

This work was supported by The Fundamental Research Funds of Shandong University (2015JC018) and Jiangsu Province Science Foundation for Youths (BK201400412).

Reference

1. V. S. Komleva, S. M. Barinova and E. V. Koplik, *Biomaterials*, 2002, **23**, 3449-3454.
2. C. Qi, Y. Zhu, C. Wu, T. Sun, Y. Jiang, Y. Zhang, J. Wu and F. Chen, *RSC Adv.*, 2016, **6**, 9686-9692.
3. D. M. Roy and S. K. Linnehanl, *Nature*, 1974, **247**, 220-222.
4. W. Paul and C. P. Sharma, *Journal of Materials Science: Materials in Medicine*, 1999, **10**, 383-388.
5. Q. He, Z. Huang, Y. Liu, W. Chen and T. Xu, *Materials Letters*, 2007, **61**, 141-143.

6. H. Yang, L. Hao, N. Zhao, C. Du and Y. Wang, *CrystEngComm*, 2013, **15**, 5760-5763.
7. C. C. Ribeiro, C. C. Barrias and M. A. Barbosa, *Journal of materials science. Materials in medicine*, 2006, **17**, 455-463.
8. P. Luo and T. G. Nieh, *Biomaterials*, 1996, **17**, 1959-1964.
9. Y. Mizushima, T. Ikoma, J. Tanaka, K. Hoshi, T. Ishihara, Y. Ogawa and A. Ueno, *Journal of controlled release : official journal of the Controlled Release Society*, 2006, **110**, 260-265.
10. R. Sun, Y. Lu and K. Chen, *Materials Science and Engineering: C*, 2009, **29**, 1088-1092.
11. T. S. Pradeesh, M. C. Sunny, H. K. Varma and P. Ramesh, *Bulletin of Materials Science*, 2005, **28**, 383-390.
12. C. Takai, T. Hotta, S. Shiozaki, Y. Boonsongritb and H. Abe, *Chemical communications*, 2009, **37**, 5533-5535.
13. R. Sun, Y. Lu, M. Li, S. Li and R. Zhu, *Surface and Coatings Technology*, 2005, **190**, 281-286.
14. X. Cheng, Q. He, J. Li, Z. Huang and R. Chi, *Crystal Growth & Design*, 2009, **9**, 2770-2775.
15. Y. Wang, M. S. Hassan, P. Gunawan, R. Lau, X. Wang and R. Xu, *Journal of colloid and interface science*, 2009, **339**, 69-77.
16. Z. Shi, X. Huang, Y. Cai, R. Tang and D. Yang, *Acta biomaterialia*, 2009, **5**, 338-345.
17. R. Sun and Y. Lu, *Frontiers of Materials Science in China*, 2008, **2**, 95-98.
18. Y. Qi, J. Shen, Q. Jiang, B. Jin, J. Chen and X. Zhang, *Advanced Powder Technology*, 2015, **6**, 1041-1046.
19. D. Bayraktar, A. C. Tas, *Journal of the European Ceramic Society*, 1999, **19**, 2573-2579.
20. R. Sun, K. Chen, Z. Liao and N. Meng, *Materials Research Bulletin*, 2013, **48**, 1143-1147.
21. H. Zhang, and B. W. Darvell, *Journal of the European Ceramic Society*, 2010, **30**, 2041-2048.
22. M. Aizawa, A. E. Porter, S. M. Best and W. Bonfield, *Biomaterials*, 2005, **26**, 3427-3433.
23. H. Zhang, Y. Wang, Y. Yan and S. Li, *Ceramics International*, 2003, **29**, 413-418.
24. M. Aizawa, F. S. Howell, K. Itatani, Y. Yokogawa, K. Nishizawa, M. Toriyama and T. Kameyama, *Journal of the Ceramic Society of Japan*, 2000, **108**, 249-253.
25. I. S. Neira, Y. V. Kolen'ko, O. I. Lebedev, G. V. Tendeloo, H. S. Gupta, F. Guitiań and M. Yoshimura, *Crystal Growth & Design*, 2009, **9**, 466-474.
26. Y. Wu, Y. Lee and H. Chang, *Materials Science and Engineering: C*, 2009, **29**, 237-241.
27. H. Zhang, Q. Zhu and Y. Wang, *Journal of Materials Chemistry*, 2005, **17**, 5824-5830.
28. N. Spanos, P. G. Klepetsanis and P. G. Koutsoukos, *Journal of colloid and interface science*, 2001, **236**, 260-265.
29. E. Boanini, P. Torricelli, M. Gazzano, R. Giardino and A. Bigi, *Biomaterials*, 2006, **27**, 4428-4433.
30. R. Sharma, R. R. Pandey, A. A. Gupta, S. Kar and M. Dhayal, *Materials Chemistry and Physics*, 2012, **133**, 718-725.
31. A. C. Tas, *Powder Diffraction*, 2001, **16**, 102-106.
32. T. I. Yoshio Ota, *Journal of the American Ceramic Society*, 1998.
33. J. Zhan, Y. Tseng, J. C. C. Chan and C. Mou, *Advanced Functional Materials*, 2005, **15**, 2005-2010.
34. K. Lin, J. Chang, Y. Zhu, W. Wu, G. Cheng, Y. Zeng and M. Ruan, *Crystal Growth & Design*, 2009, **9**, 177-178.
35. A. Bigi, G. Cojazzi, M. Gazzano, A. Ripamonti and N.Roveri, *Journal of Inorganic Biochemistry*, 1990, **40**, 293-299.
36. B. Viswanath and N. Ravishankar, *Biomaterials*, 2008, **29**, 4855-4863.
37. R. J. Dekker, J. D. de Bruijn, M. Stigter, F. Barrere, P. Layrolle and C. A. van Blitterswijk, *Biomaterials*, 2005, **26**, 5231-5239.
38. O. Suzuki, S. Kamakura, T. Katagiri, M. Nakamura, B. Zhao, Y. Honda and R. Kamijo, *Biomaterials*, 2006, **27**, 2671-2681.
39. F. Ren, Y. Leng, Y. Ding and K. Wang, *CrystEngComm*, 2013, **15**, 2137.
40. G. B. M. Vignoles, D. W. Holcomb, and R. A. Young, *Calcified Tissue International* 1988, **43**, 33-40.
41. M. Jevtic, M. Mitric, S. Skapin, B. Jancar, N. Ignjatovic and D. Uskokovic, *Crystal Growth & Design*, 2008, **8**, 2217-2222.
42. A. Jungbauer, R. Hahn, K. Deinhofer and P. Luo, *Biotechnology and bioengineering*, 2004, **87**, 364-375.
43. Z. Li, Y. Su, X. Wei, C. He and D. Wang, *CrystEngComm*, 2014, **16**, 4202.
44. G. Zhang, J. Chen, S. Yang, Q. Yu, Z. Wang and Q. Zhang, *Materials Letters*, 2011, **65**, 572-574.
45. M. J. Lochhead, S. R. Letellier and V. Vogel, *The Journal of Physical Chemistry B*, 1997, **101**, 10821-10827.
46. S. Koutsopoulos and E. Dalas. Koutsopoulos, *Journal of Crystal Growth*, 2000, **217**, 410-415.
47. J. V. Garcia-Ramos, P. Carmona and A. Hidalgo, *Journal of colloid and interface science*, 1981, **83**, 479-484.
48. M. Akinc and D. Sordele, *Advanced Ceramic Materials*, 1987, **2**, 232-238.
49. A. Celikkaya and M. Akinc, *Journal of the American Ceramic Society*, 1990, **73**, 2361-2365.
50. A. Celikkaya and M. Akinc, *Journal of the American Ceramic Society*, 1990, **73**, 245-250.
51. K. Tomoda, H. Ariizumi, T. Nakaji and K. Makino, *Colloids and surfaces. B, Biointerfaces*, 2010, **76**, 226-235.
52. M. L. Panchula and Mufit Akinc, *Journal of European Ceramic Society*, 1996, **16**, 833-841.
53. C. C. Wagner and E. J. Baran, *Journal of Raman Spectroscopy*, 2004, **35**, 395-400.
54. H. Zhang and B. W. Darvell, *Acta biomaterialia*, 2010, **6**, 3216-3222.
55. J. S. Lee and J. K. Park., *Ceramics International*, 2003, **29**, 271-278.

Carbonated porous hydroxyapatite microspheres with average diameter of about 64 μm and interconnected pores were hydrothermally synthesized by a one-step method.